Available online at www.sciencedirect.com
ScienceDirect
Proceedings of the Combustion Institute 32 (2009) 3139–3146
Proceedings of the Combustion Institute
www.elsevier.com/locate/proci

Studies on low-intensity oxy-fuel burner

Narayanan Krishnamurthy [a], P.J. Paul [b,*], Wlodzimierz Blasiak [a]

[a] Division of Energy and Furnace Technology, Royal Institute of Technology, Stockholm (KTH), Sweden
[b] Combustion Gasification and Propulsion Laboratory, Department of Aerospace Engineering, Indian Institute of Science, Karnataka, Bangalore 560012, India

Abstract

This paper presents experimental and computational results of oxy-fuel burner operating on classical flame and flameless mode for heat release rate of 26 kW/m^3. The uniqueness of the burner arises from a slight asymmetric injection of oxygen at near sonic velocities. Measurements of temperature, species, total heat flux, radiative heat flux and NO_x emission were carried out inside the furnace and the flow field was computationally analyzed. The flame studies were carried out for coaxial flow of oxygen and fuel jets with similar inlet velocities. This configuration results in slow mixing between fuel and oxygen and the flame is developed at distance away from the burner and the flame is bright/white in colour. In the flameless mode a slight asymmetric injection of the high velocity oxygen jet leads to a large asymmetric recirculation pattern with the recirculation ratio of 25 and the resulting flame is weak bluish in colour with little soot and acetylene formation. The classical flame in comparison is characterised by soot and acetylene formation, higher NO_x and noise generation. The distribution of temperature and heat flux in the furnace is more uniform with flameless mode than with flame mode.
© 2009 The Combustion Institute. Published by Elsevier Inc. All rights reserved.

Keywords: Flameless oxy-fuel combustion; Internal recirculation; Oxy-fuel combustion

1. Introduction

In many industrial processes heating can be enhanced by replacing some or all of the air with oxygen. The combustion with oxygen is called oxy-fuel combustion. The general benefits of oxygen enhanced combustion are increased productivity, higher thermal efficiencies, improved flame characteristics (in terms of higher turndown ratio, increased flame stability, better ignition characteristics), lower exhaust gas volumes, higher heat transfer efficiencies [1]. The detailed studies on oxy-fuel combustion were carried out by International Flame Research Foundation (IFRF) dealing with the various aspects like development of measuring equipments, characterisation, CFD development and validation [2,3]. To have both higher efficiencies and lower emissions in furnaces, combustion can be carried out using highly preheated air (950–1100 °C) from exhaust flue gas recovery and by suitable mixing of the fuel, air and flue gas (internal recirculation). The expectation is that the active reactant concentration becomes so low that combustion is not initiated until mixing process is complete. When the local temperature is higher than the auto-ignition temperature of the mixture, reactions proceed in a diluted/distributed manner, helping the reduction in the spatial and temporal gradients in concentration and temperature. The flame of such combus-

* Corresponding author. Fax: +91 80 23601692.
E-mail address: paul@cgpl.iisc.ernet.in (P.J. Paul).

1540-7489/$ - see front matter © 2009 The Combustion Institute. Published by Elsevier Inc. All rights reserved.
doi:10.1016/j.proci.2008.08.011

tion process is invisible and is called as flameless combustion/MILD/HiTAC/Flameless oxidation [4].

Kim et al. [5] have experimentally investigated the effect of NO emission characteristics in oxy-fuel with external flue gas recirculation for various burner configurations. The studies show the burner with stability and the flame length for different external recirculation rates. However the practical implementation of large external recirculation of high temperature flue gases would be complex. There is a scarcity of comprehensive experimental data in semi industrial and full scale combustion systems combined with the limited capabilities of measurement and CFD simulations for oxy-fuel computations [6]. Hedley et al. [7] operated oxy-fuel flames in two modes, namely, high velocity oxygen jet entraining the fuel and vice versa (reverse firing) and found that the NO_x emission was lower in reverse firing. Kobayashi et al. [8–10] in their work tested several diluted oxygen combustion (DOC) burners that yields NO_x levels of about 5 mg/MJ range for high temperature applications. They found the NO_x emission to increase with increase furnace nitrogen content and furnace temperature, but remained relatively insensitive to fuel injection velocity and firing rate.

Though there is some information on commercial use of flameless combustion [11], there is no systematic study of the combustion and emission phenomenon of such systems and hence this paper considers this aspect in detail. It characterizes the oxy-fuel combustion in the flame and flameless modes under the same conditions of power input (200 kW) and furnace temperatures (1473 K). The uniqueness of the flameless mode is the fact that oxygen injection velocities are near sonic and the slight asymmetric location of the oxygen jet leads to a substantial asymmetry in the flow field. Experiments and computations were used for studying the various parameters like temperature, flow field, intermediate species (like acetylene, ethylene), soot formation, total heat flux, radiative heat flux and NO_x emissions.

2. Flameless: air and oxy-fuel burner

Different burner configurations used in the previous studies for flameless air combustion are shown in Fig. 1. All studies have invariably used pipes for fuel and air except for configuration-1 that uses closed channel for air. For configuration-1 the air supply is in the centre and with outer two fuel jets [12]. In configuration-2 there are six sets of air nozzles with a central fuel jet and at any point of time three sets supply the preheated air (forward flow) from the regenerators and three pairs exhaust the flue gaseous (reverse flow)[13]. For effective preheating of the regenerators and consequently the combustion air periodic switching between regenerators/burners take place in configurations-1 and -2. Configuration-3 uses non-preheated air with alternate jets of air and fuel with the recirculation aided by an inner conical structure [14]. In Configuration-4 precombustor in place of regenerators for supply of preheated air has been used [15].

Flameless oxy-fuel burner used in this study is the configuration-5 shown in Fig. 1. Fu-wei-Biao et al. [16] used a similar configuration for coal flame stabilization. They have reported higher internal flue gas recirculation, brighter flame, higher turbulent intensity, flame temperatures and noise. The burner used for the flame mode study is a coaxial three pipe construction similar to that used in IFRF studies [2,3] and in industry. The fuel pipe diameter of 6 mm (inner most) and oxygen supplied through the space between outer two pipes of diameter 19 and 24 mm. For the flameless mode oxygen was separately injected through two pipes of 4 mm diameter.

3. Experimental set up and computation

3.1. Furnace set up

A horizontal cylindrical furnace with an internal volume (length = 4.5 m, diameter = 1.5 m) of 7.9 m^3 was used for the study (Fig. 2). The furnace interior is three layer insulated (from the hot side: Saffil fibre modules 50 mm, SuperG ramming mix 200 mm, G-23 insulating brick: 115 mm). There are six conical openings (to enable measurements also at angle) on the circular wall, two openings on vertical wall on both sides of the burner plate and one close to furnace exhaust. The openings are normally blocked with ceramic fibre blocks. The positions of conical openings are 360, 1116

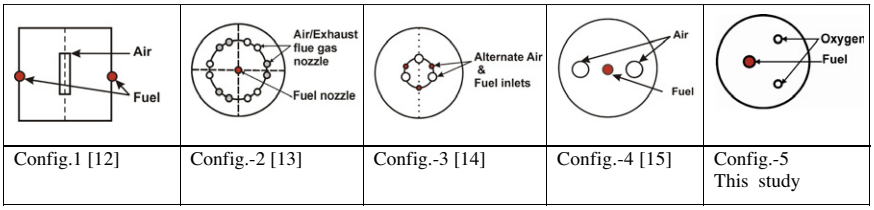

Config.1 [12]	Config.-2 [13]	Config.-3 [14]	Config.-4 [15]	Config.-5 This study

Fig. 1. Flameless burner configurations.

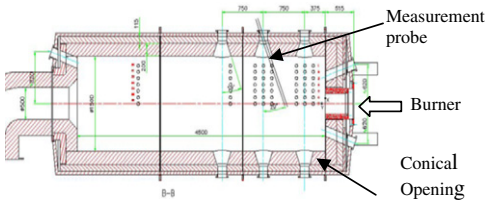

Fig. 2. Cross section of furnace showing the openings for measurement.

and 1862 mm, from the burner face. The burner is mounted on the vertical wall with the axis coinciding with the furnace axis. The fuel used was propane (200 kW) and oxidizer was pure oxygen from evaporated liquid oxygen (oxygen in chimney ~3%.). The furnace wall temperature stabilized at 1200 °C ∓ 20 °C after 16 h of firing. The furnace temperature is an average of 16 S type ceramic covered thermocouples placed 20 mm below the insulation on the upper circumference. The inside furnace temperatures were measured using a suction pyrometer (S type thermocouple), the radiative heat flux and total heat flux using IFRF probes [17]. The measurements were done at horizontal axial plane at the same height of burner. A water-cooled gas-sampling probe was inserted in the furnace to extract gas at different points and the composition was analysed using a micro gas chromatograph (including CO, C_3H_8, UHC, CO_2, O_2). The uncertainty analysis was carried out using the method of Kline and Mcclintock [18]. The accuracy of thermocouple was 8 °C at 1300 °C. The minimum and maximum uncertainties in flue gas temperature were 2.2% and 5.7%.The minimum and maximum uncertainties in heat fluxes were 2% and 6%. The uncertainties in the flue gas composition measurements were 1%. To ensure the repeatability of measurements under identical operating conditions three individual tests were performed and averaged. The standard deviation in flame temperature, total heat flux, radiative heat flux were 4%, 6.5%, 2%. The minimum and maximum standard deviations for repeatability of the flue gas composition were 4% and 8%.

3.2. Computations

The aim of the computational study was to quantify the recirculation rates, predict the flow field and combustion behavior inside the furnace. The commercial computational software package-CFX-11 was used. The standard κ–ε model was used for turbulence. The turbulent combustion was modeled using eddy dissipation concept. Propane–oxygen reacting to form equilibrated products was used. The soot prediction was done using Magnussen's model [19]. The radiation model used was differential approximation or P1-Grey model and it is a simplification of radiation transport equation and assumes radiation intensity to be isotropic [20].

The geometry of the flame mode was axis symmetric and therefore computations were performed for one twelfth part of the domain with 0.7 million nodes. The number of nodes used for the flameless mode study was 2.4 million for 180° symmetry. To obtain grid independent results a grid resolution study has been conducted upto 1 million for the flame mode and 3 million nodes for flameless. The results were within 1% for all the nodes beyond 0.5 million for flame mode and 1.5 million for flameless.

4. Results and discussion

4.1. Appearance

The distinction in 'flame' appearance between burners operated on flame and flameless mode is shown in Fig. 3. In the classical flame mode the appearance of the 'flame' is luminous and opaque and is almost white in colour, while in the flameless mode it is barely visible and is bluish in colour similar to what is reported with high intensity MILD burner [14].

4.2. Temperatures in flame

The centre line (Fig. 4) and the radial line temperature (Fig. 5) are meant to compare measured

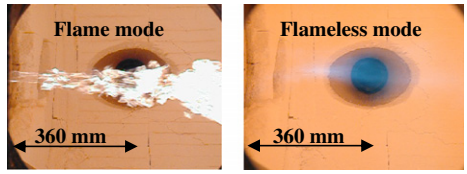

Fig. 3. Flame and Flameless mode appearance as viewed from opening at 360 mm from burner face.

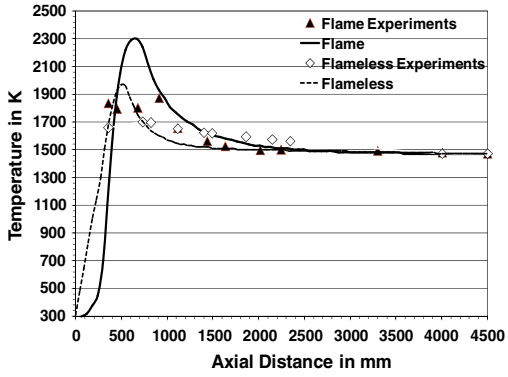

Fig. 4. Axial temperature profile measured and computed for flame and flameless mode.

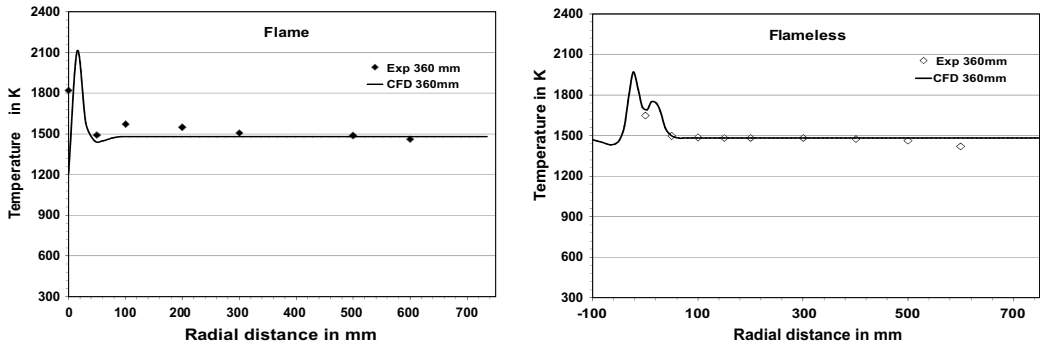

Fig. 5. Radial temperature profile of flame and flameless modes for an axial distance of 360 mm.

and computed temperatures of flame and flameless mode and to understand the effects of recirculation. The levels of accuracy of thermocouple position radially/axially are better than ±10 mm for all the locations. The diameter of the ceramic tube at tip of the suction pyrometer was 10 mm and the flue gases were sucked from the vicinity of the measurement point hence the temperature measured is an average of the region around the point of measurement. Since S type thermocouple was used it was not possible to measure the peak temperature (max measurable temperature 1873 K). The computation slightly under predicts the temperature for flameless and over predicts for flame mode as shown in Fig. 4. The peak temperature in flameless mode is ~400 K lower than flame mode. Also the temperature distribution is more uniform in the flameless mode (see also Fig. 7). In flame mode the fuel and the oxygen jets have similar velocity and hence the mixing is slow and the high intensity combustion takes place between axial distances of 300–700 mm.

4.3. Soot

During flame mode experiments soot deposition was observed on the probe surface and was very much higher than the flameless mode. The radial measurement of inflame species for flame mode at an axial distance of 360 mm from the burner face shows much higher acetylene percentage (Fig. 6) and acetylene is a known precursor for soot formation [21]. The above observations are consistent with the flame luminosity differences as reported in Section 4.1. To examine if soot can be predicted with the numerical computations, the Magnussen's soot model [19] was used. This model involves solution of two additional conservation equations for radical nuclei and soot particles. The formation of nuclei and soot particles are computed using the empirical models of Tesner et al. [22] and the combustion of nuclei and soot particles are calculated from fuel consumption reaction rate. The computed soot concentration in the flameless mode is negligible in comparison to the flame mode as shown in Fig. 8. In the flame mode soot is formed in region between the fuel and oxygen jets in the fuel rich region. Again computations are used to get an idea of temperature distribution near the burner exit region to account for the soot formation. In the flame mode the combustion commences in the shear layer between the fuel and oxygen jet immediately at the burner exit and this results in

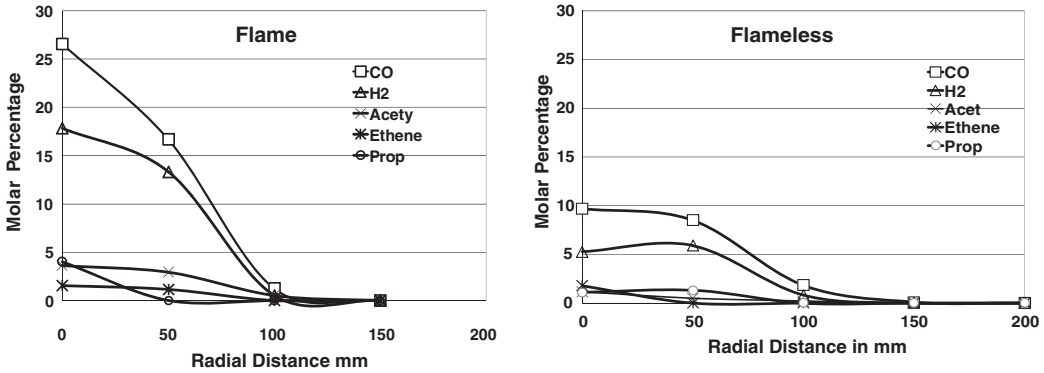

Fig. 6. Radial species profile for flame mode and flameless mode for an axial distance of 360 mm.

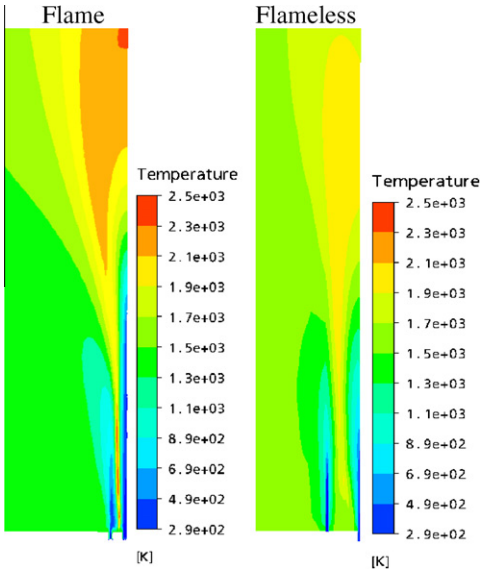

Fig. 7. Computed temperature contours on the axial plane for flame mode and flameless mode.

the fuel getting heated up to ~ 2400 K (Fig. 7). This results in pyrolysis of the fuel (slow mixing with oxygen) and favours soot formation. In the flameless mode the combination of separated injection, flue gas entrainment and dilution of incoming jets by the flue gases results in lower temperatures and consequently lower soot formation (Fig. 8). There is a qualitative agreement between average visible flame length for the flame

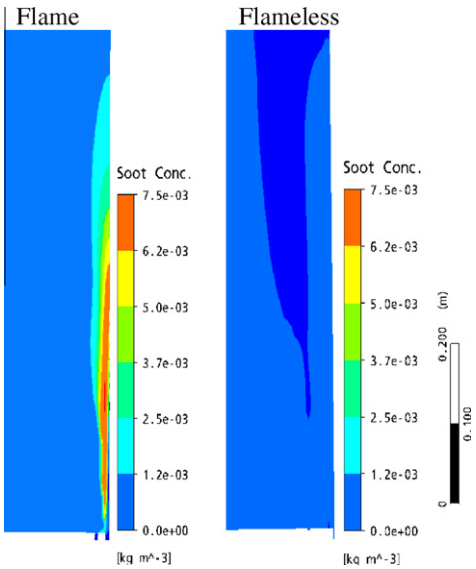

Fig. 8. Soot concentration-flame mode and flameless mode.

mode as determined from the photographs ($\sim$600 mm) and the axial extent (700 mm) of soot concentration that was computed.

4.4. Flow and recirculation

The recirculation pattern indicated by normalized velocity arrows on the axial plane for flame mode is shown in Fig. 9. To see the entrainment at the core of fuel and oxygen jet the radial profiles for an axial distance of 200 mm from the burner face is used (see Fig. 10). CO_2 which is an indicator of flue gas is not found in core of fuel jet, While CO_2 in the core of oxygen jet is both due to combustion and entrainment. The arrows show the position of core of fuel and oxygen jets.

The flow pattern for the flameless mode on the horizontal axial plane is shown in Fig. 11. The near sonic velocity oxygen injected with a slight asymmetry results in a slight deflection of the jet on one side and causes a large asymmetric recirculation of the flue gases. The reverse flow occurs on the low velocity fuel side-B. In the region close to the inlet on the side-B, the reverse flow provides the moment neutralization for both oxygen jet and the fuel jet. Additionally, the fuel jet provides the momentum neutralization for the oxygen jet. For the oxygen side-A and the gap between the oxygen and fuel jets momentum neutralization is provided by the reverse flow that is above and below the incoming jets. This low velocity reverse flow circulates the oxygen jet and fills the region between the fuel and oxygen jet till an axial distance of $\sim$150 mm from the burner face. The flow pattern is three-dimensional and causes the oxygen and the fuel jets to be diluted with the burnt gas. This description of the flow field is justified by the reasonable match of the scalar fields and the flame structure between the experiments and the calculations. Also, Fu Wei-Biao et al. [16]in their work on a similar configuration made measurements of the axial flow field and report a similar the asymmetric reverse flow structure.

The radial profiles (line connecting the core of jets) of propane, CO_2 and oxygen for an axial distance of 200 mm for flameless mode shows the presence of CO_2 at core of the both the jets shown by arrows in Fig. 10. Also, the mass fraction of CO_2 in the space between the fuel and oxygen jets is higher than equilibrated composition indicating the entrainment of flue gases.

The ratio of jet momentum for the flameless and flame mode is about 3 and a recirculation

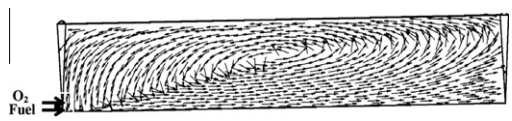

Fig. 9. Flow pattern on the axial plane for flame mode.

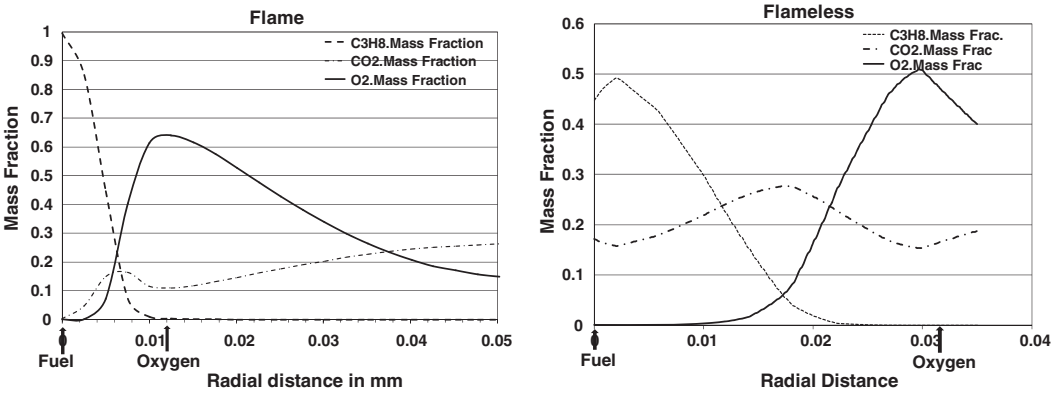

Fig. 10. Radial profiles of propane, carbon dioxide and oxygen for an axial distance of 200 mm from burner face for flame and flameless mode.

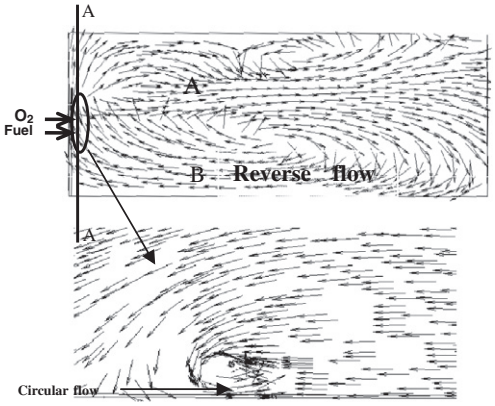

Fig. 11. Flow pattern on axial plane for flameless mode. The circular flow in the vicinity of oxygen jet is shown on a radial plane for an axial distance of 30 mm from the burner face.

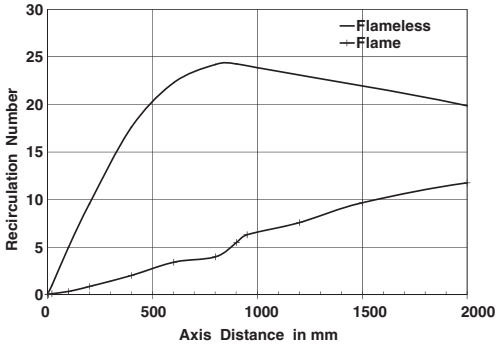

Fig. 12. Recirculation number for flame and flameless combustion shown till an axial distance of 2000 mm.

number is used to quantify the extent of recirculation. The recirculation number used here is the reverse flow obtained from computations at various cross sections normalized by the total inlet flow. At an axial distance of 200 mm the recirculation number is 0.9 (max 12) for flame mode and 10 (max 25) for flameless mode shown in Fig. 12.

4.5. NO_x emissions and noise

The burner had provisions for switching between flame and flameless modes and NO emission was measured in the chimney. Under conditions of oxy-fuel combustion, one would not expect any NO_x. Since NO_x was actually measured, there was concern about possible leakages into the system. It was found that the oxygen injection occurs at high velocities causing very low pressures adjacent to the injection zone and it was inferred that this would the cause of air ingress. The measurements inside the furnace using gas chromatography showed that the average nitrogen percentage in the region where more than 90% of NO_x is formed was 2% and 5% for the flame and flameless modes respectively. The NO_x was computed (see Table 1) using this information obtained from measurements and by taking equilibrium conditions for the reaction $O_2 \leftrightarrow 2O$ [23]. The NO_x formation rate was given by

$$\frac{d[NO]}{dt} = 2k_{N1f}[O]_{eq}[N_2] \quad \text{where}$$

$$K_{N1f} = 1.8 \times 10^{11} \exp\left[-\frac{38370}{T}\right] \ \mathrm{m^3/kmol\ s}$$

Table 1
NO_x emissions comparisons in mgs/MJ

Mode	Nitrogen	Experiments	Computations
Flame	2%	11	14.1
Flameless	5%	2	2.21

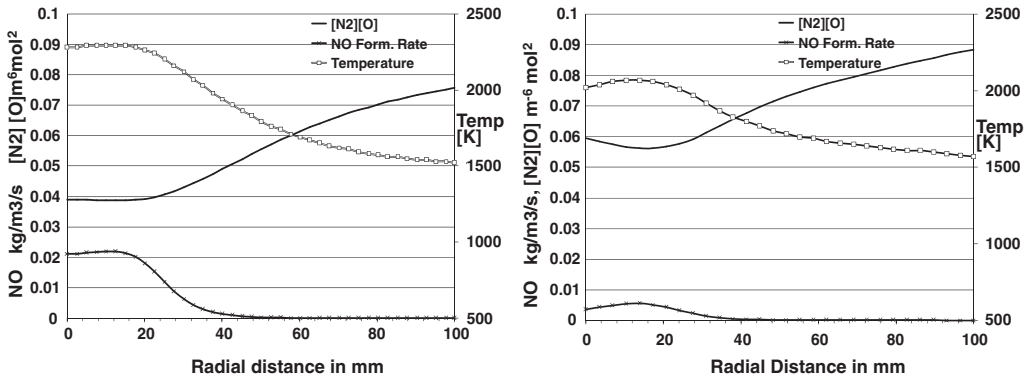

Fig. 13. Radial profiles of temperature, NO formation rate and product of molar concentration of O and N_2 for flame mode and flameless modes for an axial distance of 550 mm.

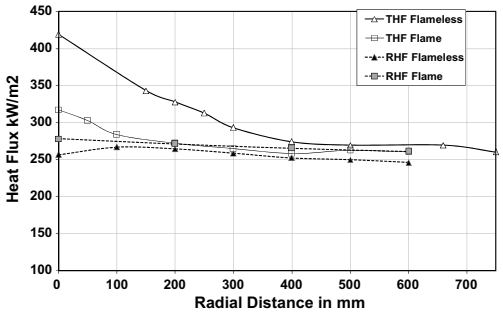

Fig. 14. Radial profiles of total heat flux (THF) and radiative heat flux (RHF) for flame and flameless modes for an axial distance of 1116 mm.

The NO_x emissions in the present work (2 mg/MJ) are consistent with the results of Kobayashi (5 mg/MJ)[9]. To compare the NO formation rates of flame and flameless mode, the radial profiles at an axial distance of 550 mm which corresponds to the regions of max NO formation rate for the flameless mode is used. The profiles show that even the peak NO formation rate is about one order magnitude lower in flameless mode as shown in Fig. 13. The noise for flameless mode was 6–9 dB lower as measured through opening close to the burner.

4.6. Total and radiative heat flux

The radial measurement of total heat flux and radiative heat flux at a axial distance of 1116 mm from the burner face is shown in the Fig. 14. The radiative heat fluxes for flame and flameless mode show similar characteristics. This is explainable as the flame radiation is only a small portion of the total heat flux and balance is from the furnace wall. The total heat fluxes measured was higher for flameless mode than for flame mode. However the flame configuration had higher heat fluxes up to an axial distance of ~400 mm from the burner face and for greater axial distance it was lower than flameless mode.

5. Conclusions

Flame and flameless oxy-fuel combustion were compared under similar conditions. The following conclusions can be drawn.

- Flameless oxy-fuel combustion can be achieved by asymmetric injection of high velocity oxygen.
- The visual appearance of 'flame' in the flame and flameless modes are distinctly different. The 'flame' is transparent blue and is hardly visible in the flameless mode, while in flame mode it is white in colour.
- The soot formation is negligible in flameless and is higher in flame mode. Measurements show that acetylene percentage is higher in flame mode contributing to the visibility difference.
- In the flameless mode the increased internal flue gas recirculation results in a more uniform temperature distribution in the combustion chamber along with lower peak temperatures than the flame mode.
- The radiative heat fluxes profiles are similar for flame and flameless modes. The total heat flux distribution is more uniform with flameless than flame mode.
- NO_x emissions can be maintained at low or even very low levels well meeting restrictions at industrial-scale operation with flameless oxy-fuel combustion.

Acknowledgments

The authors wish to thank Linde AG (www.lindegas.com/rebox), Sweden and Hindustan Petroleum Corporation Limited, India for facilitating the research.

References

[1] C.E. Baukal, *Oxygen Enhance Combustion*, CRC Press, 1998.

[2] L.A.J. Dugue, R. Weber, Analysis of the experimental data collected during the OXYFLAME-1 and OXYFLAME-2 Experiments 1995-1996, IFRF DOC no D 85/y/4.

[3] L.A. Verlaan, R. Weber, Analysis of the experimental data collected during the OXYFLAME-3 Staged and Premixed Flames, 1996–1997, IFRF DOC no D 85/y/5.

[4] A. Cavaliere, M. de Joannon, *Prog. Energy Combust. Sci.* 30 (2004) 329–366.

[5] H.K. Kim, Y. Kim, S.M. Lee, K.Y. Ahn, *Combust. Inst.* 31 (2007) 3377–3384.

[6] U. Bollenttini, F. Breussin, N. Lallement, R. Weber, Mathematical Modelling of Oxy-Natural gas FlamesA,: IFRF DOC no F 85/y/3.

[7] J.T. Hedley, M. Pourkashanian, A. Williams, L.T. Yap, *Combust. Sci. Technol.* 108 (1995) 311–322.

[8] H. Kobayashi, Segregated Zoning Combustion, Patent 5,076,779, December 31, 1991.

[9] H.M. Ryan, A.W. Francis, M.F. Riley, H. Kobayashi, *Dilute Oxygen Combustion*, Phase I Report for U.S. Dept. of Energy (DOE/ID/13331-T1), October, 1997.

[10] M.F. Riley, H. Kobayashi, A.C. Deneys, *JOM, Miner., Metals Mater. Soc.* (2001) 21–24.

[11] <http://www.linde-gas.com/rebox>.

[12] W. Yang, M. Mortberg, W. Balsiak, *Scand. J. Metall.* 33 (2004) 1–9.

[13] J.A. Wunning, J.G. Wunning, *Prog. Energy Combust. Sci.* 33 (1997) 81–94.

[14] S. Kumar, P.J. Paul, H.S. Mukunda, *Proc. Combust. Inst.* 29 (2002) 1131–1137.

[15] M. Mancini, R. Weber, U. Bollenttini, *Proc. Combust. Inst.* 29 (2002) 1155–1163.

[16] F.W. Biao, W. Jing-Bin, Z. Huan-Qing, *Combust. Inst.* 21 (1986) 567–574.

[17] J. Chedaille, Y. Braud, *Industrial Flames, Measurement in Flames*, vol. 1, Edward Arnold (Publishers) Ltd., London, 1972.

[18] S.J. Kline, F.A. Mcclintock, *J. Mech. Eng.* 75 (1953) 3–8.

[19] B.F. Magnussen, B.H. Hjertager, *Combust. Inst.* 16 (1976) 719–729.

[20] G.D. Raithby, Progress Report, Thermal Science Ltd., 1991, Provided to EMR.

[21] I. Glassman, *Combustion*, Third edition, Academic Press, 403 pp.

[22] P.A. Tesner, T.D. Snegiriova, V.G. Knorre, *Combust. Flame* 17 (1971) 253–260.

[23] S.R. Turns, An Introduction to Combustion: Concepts and Application, Mcgraw Hill Press.